Antarctic Science (2025), **37**, 413–426
doi: 10.1017/S095410202510028X

CAMBRIDGE UNIVERSITY PRESS

Earth Sciences

Thermal regimes and phases of surface temperature in Livingston and Deception islands, Antarctica, 2007–2021: influence of snow cover and implications for frozen ground

Miguel Ángel de Pablo[1], Miguel Ramos[2,3], Gonçalo Vieira[3], Antonio Molina[4] and Jesús Ruiz-Fernández[5]

[1]Departamento de Geología, Geografía y Medio Ambiente, Facultad de Ciencias, Universidad de Alcalá, Madrid, Spain; [2]Departamento de Física y Matemáticas, Facultad de Ciencias, Universidad de Alcalá, Madrid, Spain; [3]Centro de Estudos Geográficos, Instituto de Geografia e Ordenamento do Território, Universidade de Lisboa, Lisbon, Portugal; [4]Centro de Astrobiología (CAB), CSIC-INTA, Madrid, Spain and [5]Departamento de Geografía, Universidad de Oviedo, Oviedo, Spain

Abstract

The study of the ground surface temperature (GST) regimes from 2007 to 2021 at different stations on Livingston and Deception islands, South Shetland Islands, in the north-western sector of the Antarctic Peninsula (AP), shows that soils undergo similar cooling in early winter before a shallow snow mantle covers the sites. All monitoring sites along the study period go through seasonal phases of cooling, attenuation, insulation, fusion and zero curtain during winter, although thermal equilibrium is only reached at some stations located at lower elevations on Livingston Island. GST evolution at these stations and the duration of snow periods show oscillations, with turning points in the years 2014 and 2015, when temperatures were at their minimum and snow durations were at their maximum, in agreement with the cooling period occurring in the north-western AP in the early twenty-first century. The thermal regime is mainly controlled by snow cover and its onset and offset dates based only on descriptive patterns, not on statistical testing, more than by altitudinal, topographical, geological or geomorphological factors.

Keywords: Freezing and thawing periods; ground surface temperature; South Shetland Islands, Antarctica

(Received 28 October 2024; revised 21 June 2025; accepted 11 July 2025)

Introduction

The western sector of the Antarctic Peninsula (AP) is one of the regions on Earth where temperatures have been rising rapidly in recent decades. An increase of 0.54°C in air temperature was reported in the second half of the twentieth century (Turner *et al.* 2005, 2019, Steig *et al.* 2009). Despite the cooling recorded between 2000 and 2015 in the AP (Carrasco 2013, Turner *et al.* 2016, Oliva *et al.* 2017), and considering the regional climate variability, a general increase in temperature continued in the early decades of the twenty-first century (e.g. Turner *et al.* 2016, IPCC 2019, Clem *et al.* 2020). This atmospheric warming had implications in various areas, including sea temperature, glacier mass balance, soil ecological conditions and its thermal regime and geomorphological dynamics (e.g. Meredith & King 2005, Molina *et al.* 2007, Convey *et al.* 2009, Vieira *et al.* 2010, Abram *et al.* 2013, Bockheim *et al.* 2013, Kejna *et al.* 2013, Navarro *et al.* 2013, Turner *et al.* 2013, Oliva & Ruíz-Fernández 2015, 2017, Sancho *et al.* 2017, Engel *et al.* 2018, Obu *et al.* 2020, Putzke & Pereira 2020, Auger *et al.* 2021, de Pablo *et al.* 2024).

Corresponding author: Miguel Ángel de Pablo; Email: miguelangel.depablo@uah.es

Cite this article: de Pablo, M. Á., Ramos, M., Vieira, G., Molina, A., & Ruiz-Fernández, J. 2025. Thermal regimes and phases of surface temperature in Livingston and Deception islands, Antarctica, 2007–2021: influence of snow cover and implications for frozen ground. *Antarctic Science* **37**, 413–426. https://doi.org/10.1017/S095410202510028X

As is widely known (e.g. Smith & Riseborough 2002, Romanovsky *et al.* 2010), increases in air temperatures have direct consequences on the thermal regime of soils. Considering the absence of significant vegetation cover (de Pablo *et al.* 2024), the soil thermal regime will mainly be modulated, at the local scale, by the insulating effect of snow cover (Zhang 2005), overriding other geographical and climatical factors. Understanding the daily thermal regime of soils enables the identification of the context for the development of certain periglacial processes or the conditions for vegetation growth in the harsh and limiting conditions of Antarctica (e.g. Guglielmin 2006). There are increasing numbers of studies examining the soil thermal regime in the AP (e.g. Cannone *et al.* 2006, Guglielmin 2006 and references therein, Cannone & Guglielmin 2009, Francellino *et al.* 2011, Guglielmin *et al.* 2012, 2014a,b, Roberts *et al.* 2013, Fisher *et al.* 2016, Ambrožová *et al.* 2020, Hrbáček *et al.* 2020, Obu *et al.* 2020, Lacelle *et al.* 2022, Lim *et al.* 2022, Savenets *et al.* 2023, de Pablo *et al.* 2024) due to its significant implications. With this work, we aim to study the yearly thermal regime and the thermal phases of frozen soils on Livingston and Deception islands, in the AP's western sector, where global warming's effects will first affect the surficial regime (González-Herrero *et al.* 2024). The specific research questions we intend to address in this study are: how is the ground surface thermal regime of the study areas characterized? How and when does ground cooling occur? What role does the snow cover

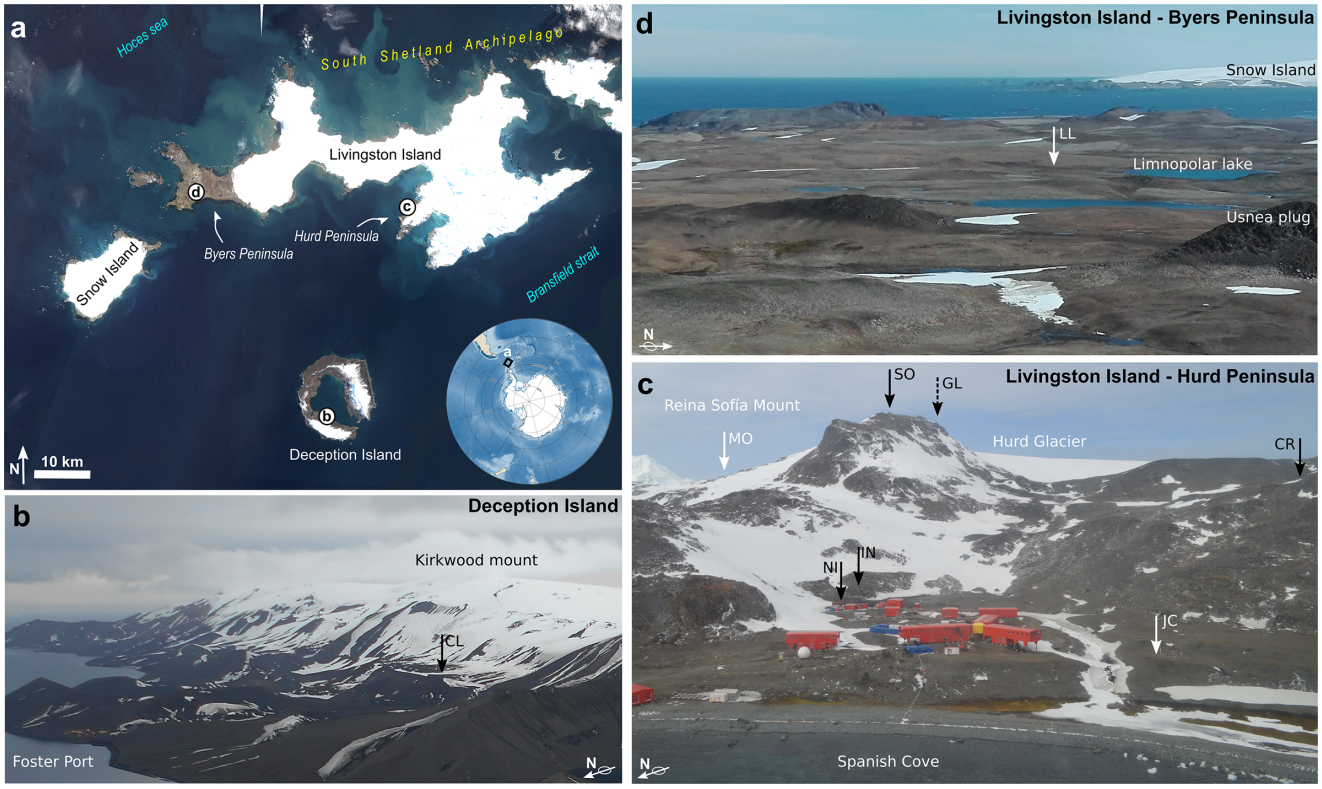

Figure 1. Locations of the ground surface temperature monitoring stations of the PERMATHERMAL network on Livingston and Deception islands, South Shetland Islands, Antarctica. **a.** Satellite view of the South Shetland Islands, showing the locations of the three study areas: **b.** Deception Island, **c.** Hurd Peninsula and **d.** Byers Peninsula on Livingston Island. **b.** Oblique view of the southern flank of Deception Island showing the location of CL station. **c.** Photograph from Spanish cove of the northern flank of Reina Sofía Mount, showing the distribution of JC, NI, IN, CR, MO and SO stations. **d.** View of the western sector of Byers Peninsula with the location of LL station.

Table I. Main settings of the ground surface temperature monitoring sites on Livingston and Deception islands (simplified from de Pablo *et al.* 2023, after Ferreira *et al.* 2017).

Location	Area	Site		Elevation (m)	Established	Geomorphology	Wind
		Name	Code				
Livingston Island	Hurd Peninsula	'Juan Carlos I' Station	JC	12	2010	Raised beaches	Low
		Nuevo Incinerador	NI	19	2007	Slope foot	Very low
		Incinerador	IN	34	2009	Rock step in slope	Low
		Collado Ramos	CR	117	2007	Wide, flat interfluve	High
		Morrena	MO	145	2009	Lateral moraine	High
		Reina Sofia Mount	SO	274	2009	Slope top near summit	Very high
	Byers Peninsula	Limnopolar Lake	LL	80	2009	Gentle slope	High
Deception Island	Crater Lake	Crater Lake	CL	85	2009	Gentle slope	Very high

play? Does the snow cover attenuate the atmospheric thermal signal? What are the consequences of the type and duration of the snow cover on soil temperatures? Is permafrost possible under these conditions? How have the ground thermal regime and the associated environmental conditions evolved over time, and what are the implications of this for the soils?

Along with answering these questions, we also aim to answer some more general inquiries: has there been a change in the thermal regime trend of soils in the area during the time period of investigation? Are these potential changes related to the cooling and warming periods recorded in the early twenty-first century in the western region of the AP?

Study areas

To address these questions, ground surface temperature (GST) data acquired at the PERMATHERMAL network stations (de Pablo 2021, 2022, 2023) are used. This network comprises various stations for ground thermal monitoring on Livingston and Deception islands, located in the South Shetland Islands archipelago in the north-western sector of the AP. GST sensors have been progressively set up among the instruments installed at the different stations since 2007. In this study, GST data from eight stations are used (Fig. 1): six are situated at elevations ranging from 12 to 274 m above sea level (a.s.l.) on Hurd Peninsula (Livingston

https://doi.org/10.1017/S095410202510028X Published online by Cambridge University Press

Island), one is on Byers Peninsula (Livingston Island) and one is on Deception Island (Table I). Each of these stations features varying geomorphological settings and exposures to prevailing winds (Table I). Nonetheless, the site selection aimed to represent typical environmental conditions and windy exposures (de Pablo *et al.* 2024). The use of several stations in Hurd Peninsula aims to assess altitudinal and geomorphological effects, as this area shows more significant geomorphological and geological variability compared to Byers Peninsula and Deception Island (Table I).

Both islands have a cold maritime climate at sea level, with mean annual air temperatures (MAATs) ranging from −2°C to −1°C (Bañón 1994, 2001, Ramos *et al.* 2008b, Bañón & Vasallo 2015). MAAT decreases with increasing elevation, reaching as low as −4°C at Reina Sofía Mount (Ramos *et al.* 2008a). Annual precipitation, primarily as snow, is ~500 mm at sea level, with greater accumulation during spring, although liquid precipitation is expected at low elevations, typically below 100 m a.s.l., during summer (Bañón *et al.* 2013). Winds exhibit a variety of directions, with the south-westerly prevailing at an annual average speed of ~25 km/h, occasionally peaking at 140 km/h (Bañón *et al.* 2013).

A seasonally freezing and thawing surface layer occurs at all stations, with thicknesses ranging from 40 to 160 cm depending on the island and elevation (de Pablo *et al.* 2013, 2014, 2024, Hrbáček *et al.* 2016a,b, Ramos *et al.* 2017). Permafrost is absent from low-elevation sites (Ferreira *et al.* 2017), with the limit between continuous and discontinuous permafrost occurring at ~150 m a.s.l. in the Hurd Peninsula (Ramos *et al.* 2013). At Reina Sofía Mount, permafrost is at least 25 m thick (Ramos & Vieira 2009, Ramos *et al.* 2020), whereas permafrost is widespread on Deception Island, with thicknesses varying from 3 to 25 m (Vieira *et al.* 2008, Bockheim *et al.* 2013, Ramos *et al.* 2013, 2017, Goyanes *et al.* 2014). Climatic and geophysical data suggest that permafrost on these islands is near its thermodynamic limit of existence (Hauck *et al.* 2007, Vieira *et al.* 2010, Bockheim *et al.* 2013, de Pablo *et al.* 2024).

Data and methods

Ground surface temperature monitoring

GST has been measured continuously since 2009 at eight monitoring stations of the PERMATHERMAL network, with testing also occurring since 2007 at three stations (NI, CR and MO; Fig. 1, and see Table I for station naming codes), using iButton Thermochron DS1921G devices with 0.5°C resolution and accuracy, measuring every 4 h. In 2009, the instruments at all stations were upgraded the DS1922L devices with a resolution of 0.0625°C and an accuracy of 0.5°C. These devices, capable of storing up to 4096 measurements, were programmed to measure every 3 h to ensure data collection for a full year. The instruments were attached by means of a plastic support model DS9093F+ to a duralumin or stainless-steel plate of 20 × 20 × 0.2 cm to obtain more representative GSTs. The plates were buried ~2–3 cm deep to prevent their direct heating by solar radiation or their direct cooling by snow and ice. Data were downloaded annually, generally in January or February, by taking the sensors from the plates, and the plates were then reinstalled again after programming the devices for a new year of data acquisition (de Pablo *et al.* 2024).

Data processing

Despite continuous monitoring, there are gaps in the time series due to 1) failure of the devices caused by battery exhaustion, 2) damage due to moisture and 3) memory capacity being reached due to logistical complications in site access. These gaps have not been filled using any algorithm, so the analysis of the available data was performed as the data stood. Data from each sensor were processed as follows (de Pablo 2021, 2022, 2023, de Pablo *et al.* 2024): 1) elimination of invalid data recorded at the beginning or end of each file, 2) deletion of erroneous data (temperatures outside the working range) and 3) 0°C calibration using the zero-curtain period (Outcalt *et al.* 1990) and the latest data of the previous year. This last correction always implied offset values lower than the precision of the devices (± 0.5°C).

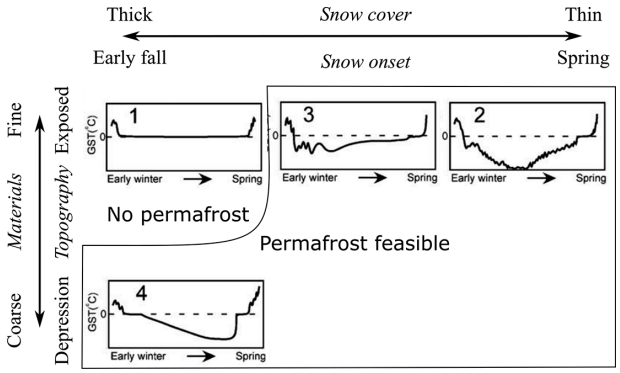

Figure 2. Typical ground surface temperature (GST) thermal regimes in cold regions and the main parameters controlling them to allow for the presence of permafrost (permafrost feasible, possible and/or probable; based on Ishikawa 2003).

Thermal regime classification

Depending on the general annual behaviour of GST, we define the yearly thermal regime at each station using the classification of Ishikawa (2003), which depends on when soil freezing occurs, based on the date of snow cover onset (Fig. 2). We recognize the following main types:

- Regime Type 1: no soil freezing due to the presence of thick snow cover from late summer
- Regime Type 2: ground cooling throughout the winter due to absent or very thin snow cover
- Regime Type 3: ground cooling before the accumulation of an insulating snow cover layer
- Regime Type 4: ground cooling due to air flow through the granular soil materials

We studied the temporal evolution of the ground thermal regimes over time at each station in terms of elevation and location.

Phases of the ground surface thermal regime

The time series were plotted to determine the duration of the GST periods (Fig. 3), following the definitions of Delaloye (2004) and Schoeneich (2011), as follows:

- Phase 1: warming. Characterized by positive temperatures (except in short periods), corresponding to the summer season when the ground warms up.
- Phase 2: cooling. Temperatures drop below 0°C, although there may be episodes of higher temperatures and even curtain effect periods associated with the first autumn snowfalls. In this phase,

https://doi.org/10.1017/S095410202510028X Published online by Cambridge University Press

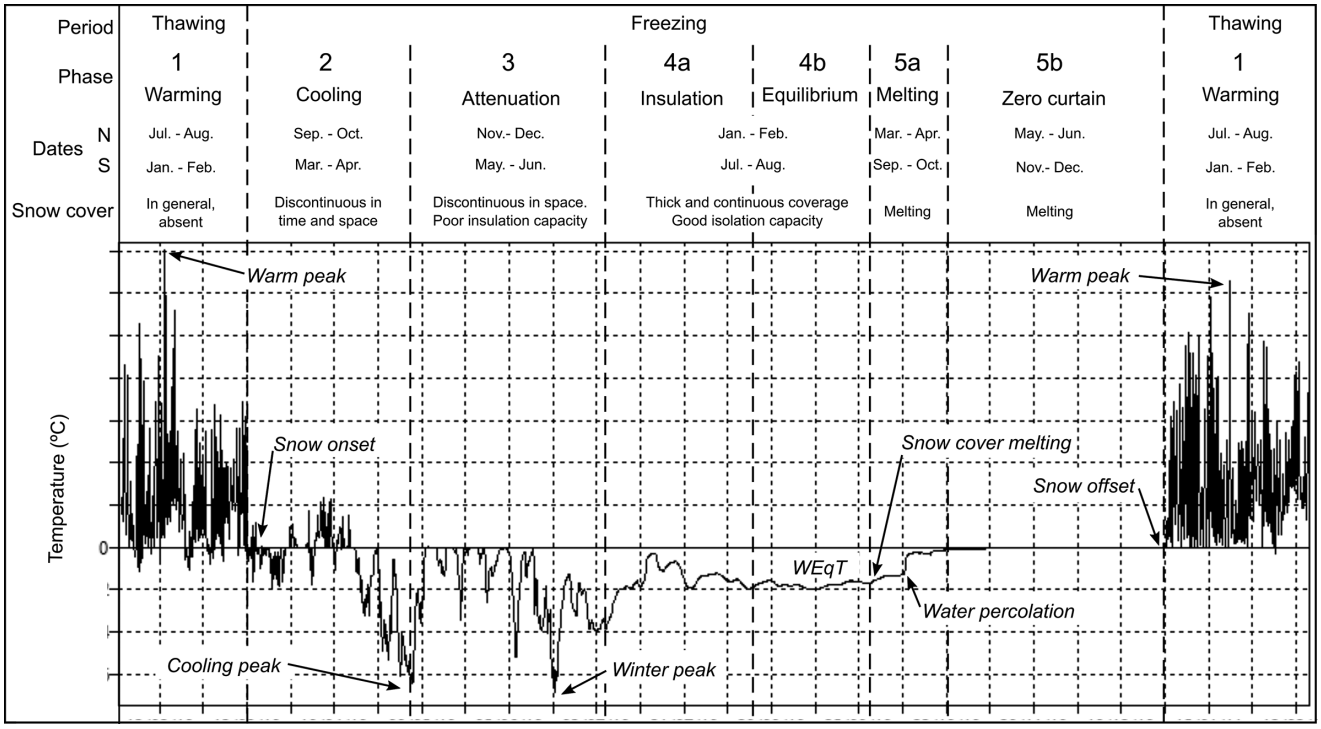

Figure 3. Theoretical diagram of the phases of thermal evolution of seasonally frozen soils (modified from Delaloye 2004, Schoeneich 2011). WEqT = equilibrium temperature.

temperatures decrease significantly, and daily thermal variability is maintained.

- Phase 3: attenuation. The snow cover is now sufficient to provide some insulation for the ground, resulting in reductions in the daily thermal variability.
- Phase 4a: insulation. The snow cover has reached sufficient thickness to insulate the ground significantly, resulting in only long-term temperature fluctuations, and the temperature is controlled by the temperature of the snow and of the permafrost table, when present.
- Phase 4b: equilibrium. The thickness and duration of the snow mantle are sufficient to provide insulation, allowing the terrain to maintain a very regular equilibrium temperature (WEqT) with minimal long-term variation.
- Phase 5a: melting. Snow cover begins to melt, and temperatures start to rise significantly. When meltwater percolates through the snow layer and reaches the ground, there is a significant increase in temperatures before the curtain effect period, which usually occurs before the complete disappearance of the snow.
- Phase 5b: zero curtain. This phase is characterized by isothermal conditions of ~0°C as the ground thaws, known as the 'curtain effect' (Outcalt *et al.* 1990), preceding the summer warming phase.

It is important to clarify that in the division into thermal phases of the soils, Delaloye (2004) initiates Phase 5 (here Phase 5a) when significant warming occurs before the onset of the curtain effect associated with the arrival of infiltration water into the ground. However, in Schoeneich (2011), the boundary between these phases is defined as when temperatures indicate that the ground has exited the insulation and/or equilibrium phase and is beginning to increase in temperature gradually. In this work, we follow the latter criterion while providing the date of occurrence of the former (Table II) to enable future comparative studies by other authors. Furthermore, neither Delaloye (2004) nor Schoeneich (2011) distinguishes the subphases in the melting process. We have chosen to define two subphases to emphasize the presence and duration of the curtain effect period, which is crucial when studying snow presence and its relative thickness. Finally, we have calculated the total duration of the thawing (Phase 1) and freezing periods (Phases 2, 3, 4a, 4b, 5a and 5b) for each annual cycle, which often exceeds a natural year. This allowed us to assess its annual evolution.

Distinguishing between the different phases was performed visually (Table II). The cases of the separation between Phases 1 and 2 and between Phases 5b and 1 are quite clear due to the sharp changes in thermal behaviour; in other cases, such as between Phases 3 and 4 or even between Phases 4a and 4b, distinguishing between them is more subjective and so potentially disputable. We reviewed each yearly dataset recursively to ensure that the same criteria were applied in all cases by the same researcher. Establishing a mathematical method based on daily thermal amplitude changes over time or even the defining such thresholds has not been attempted in the literature and will be the objective of future works.

Extreme temperatures and equilibrium temperatures

The dates and values of the maximum temperatures recorded during the ground warming period have been identified (Table II), as well as those of the minimum temperatures during the cooling and attenuation phases. Additionally, when applicable, the equilibrium temperature, or WEqT, was determined. WEqT has been used as a reference for assessing the likelihood of permafrost presence beneath the active layer, similar to the bottom temperature of snow cover (BTS) methodology (Haeberli 1973, 1985, King 1983), with the following limits (Hoelzle 1992):

https://doi.org/10.1017/S095410202510028X Published online by Cambridge University Press

Table II. Definition of the starting dates of the different key periods in the thermal evolution of seasonally frozen soils (following Delaloye 2004, Schoeneich 2011) and key temperatures.

Parameter	Definition
First snow	Date of the arrival of the first snowfall, with a non-permanent and irregularly distributed pattern
Snow onset	Date when the snow definitively covers the terrain until spring. Drop in temperatures below 0°C until the end of the freezing period. Boundary between Phases 1 and 2
Cooling	Date when the period starts with drastic temperature decreases below 0°C, but with daily thermal fluctuations. Boundary between Phases 2 and 3
Cooling peak	Date of the lowest temperatures during the cooling period or Phase 3
Insulation	Date when the period of low temperatures begins to attenuate. Boundary between Phases 3 and 4a
Winter peak	Date of the lowest temperatures during the isolation period or Phase 4a
Snow melting	Date when temperatures start rising at the end of Phase 4. Boundary between Phases 4 and 5
Water percolation	Date of the sudden rise in temperatures at the end of the freezing period, or Phase (4), before reaching the zero-curtain period
Zero curtain	Date when temperatures reach a value close to 0°C and remain approximately constant for a time period
Snow offset	Date when temperatures turn positive again at the end of the freezing period or Phase 4, and the zero-curtain period. Boundary between Phases 5 and 1. Start of the warming phase
Warm peak	Date of the maximum temperature during the thawing period or Phase 1
Warm peak temperature	Maximum temperature (°C) during the warming phase or Phase 1
Cooling peak temperature	Minimum temperature (°C) during the cooling phase or Phase 2
Winter peak temperature	Minimum temperature (°C) during the attenuation phase or Phase 3
WEqT	Equilibrium temperature (°C) reached in Phase 4b, when reached
Freezing period	Freezing period (in days), defined between the cooling, attenuation, insulation, equilibrium, melting and zero-curtain periods
Thawing period	Thawing period (in days), corresponding to the warming period
Snow-free period	Snow-free period (in days), defined between snow offset and snow onset
Snow period	Period (in days) with snow cover, defined between snow onset and snow offset

- WEqT < −3°C: permafrost likely
- -2°C > WEqT > −3°C: permafrost possible
- WEqT > −2°C: permafrost unlikely

Snow cover

The presence of snow has been determined based on GST analysis following Danby & Hik (2007). According to this method, when the daily temperature variance is <1°C, the ground is considered to be covered by snow. The first time this variance persists for 3 consecutive days at the end of summer or early autumn, the snow period commences (i.e. snow onset). It ends when this variance exceeds the 1°C threshold at the end of winter or the beginning of spring (i.e. snow offset). The duration of the snow period is calculated as the number of days between snow onset and snow offset (Table II).

It is important to note that the snow offset corresponds to the end of the curtain effect period and the beginning of the warming phase, as previously defined in this study. Additionally, the duration of the snowmelt period has been calculated as the number of days between the start of the melting phase (Phase 5a) and the snow offset (end of Phase 5b; Table II).

Results and interpretation

Thermal regimes

The temperatures recorded at all stations throughout the study period (2007–2021) exhibit clear seasonality with two major periods. Firstly, during the summer periods, temperatures consistently remain above 0°C. Secondly, during the winter periods, temperatures do not exceed this threshold (Fig. 4). There is no instance in which GST at the stations remained above 0°C or in a zero-curtain phase throughout the entire winter period. Nor have there been stations where temperatures did not undergo thermal attenuation during winter, indicating the presence of a certain thickness of snow cover with insulating properties.

Therefore, based on the observed thermal behaviour, it can be established that all stations have exhibited a Type 3 thermal regime (Ishikawa 2003). According to this classification, the ground cools before the arrival of a snow cover with sufficient thickness to at least attenuate the thermal signal from the atmosphere. This seasonal structure is recognizable in the GST curves shown (Fig. 4), in which cooling begins before attenuation stabilizes temperatures. In many cases, soil insulation is achieved, although equilibrium (WEqT) during the winter is only reached in a few cases, as we will discuss later. Despite the uniformity in the thermal regimes of all stations, station LL shows a pattern that is more consistent with a Type 4 regime, characterized by partial insulation and moderate thermal damping during winter. Similarly, station NI has experienced limited cooling in the early autumn and quickly enters a zero-curtain phase extending for up to 5 months, leaning towards a Type 1 regime, but without becoming distinctly Type 1. For example, some stations take longer to attenuate the daily thermal signal, but at no point does it persist throughout the entire winter, preventing the achievement of a complete Type 2 thermal regime.

https://doi.org/10.1017/S095410202510028X Published online by Cambridge University Press

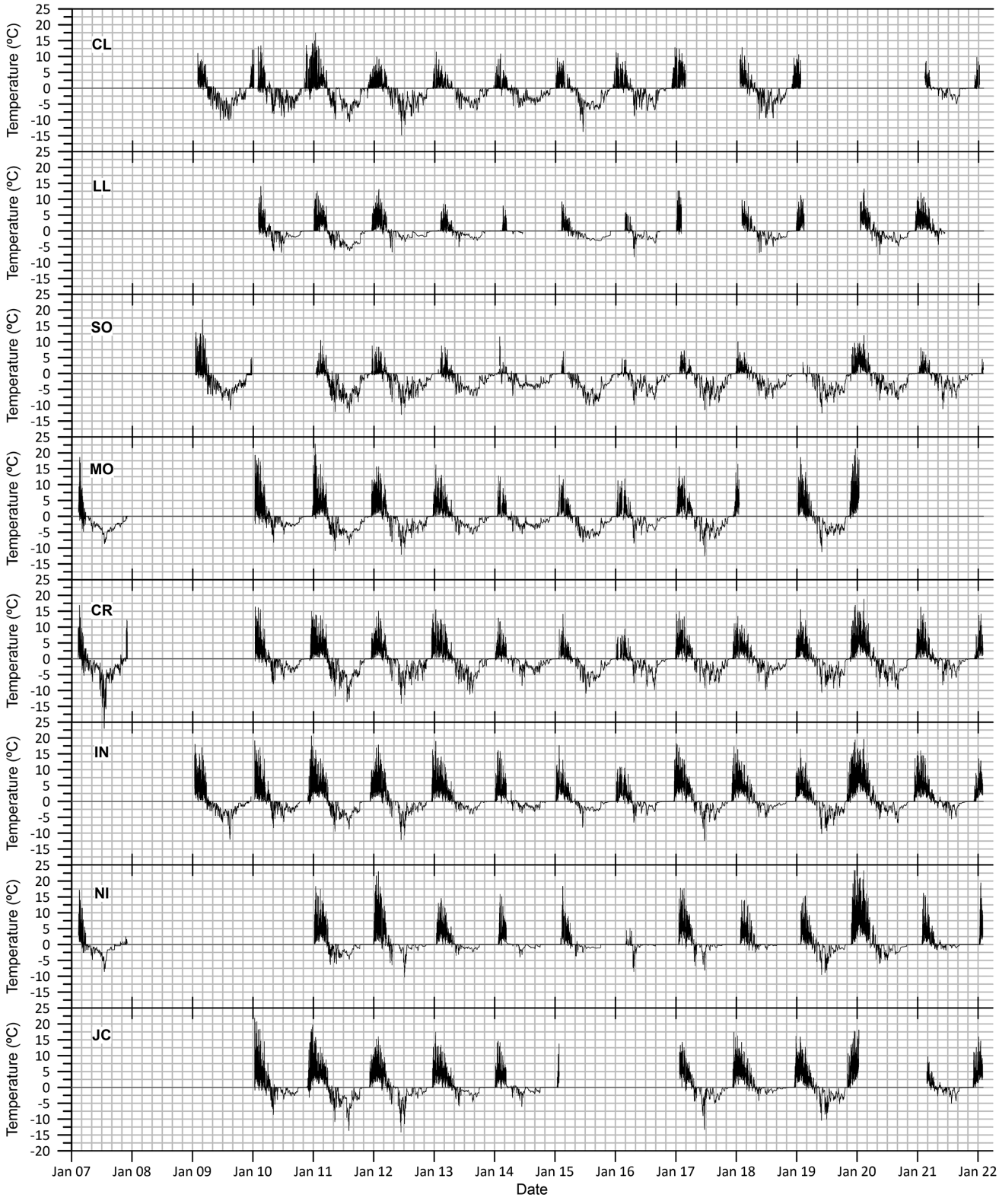

Figure 4. Ground surface temperatures at all monitoring stations (letter codes as in Table I) during the 2007–2021 period.

Thermal phases

The analysis of thermal phases (Fig. 3) in GST across all stations reveals a certain uniformity among them (Table III). Typically, stations go through a thawing phase (Phase 1), followed by a cooling process (Phase 2) at the beginning of autumn, succeeded by an attenuation period (Phase 3) when the snow cover begins to thicken and provide insulation. Subsequently, they progress to the insulation phase (Phase 4a) when the snow cover becomes highly insulating. In only a few cases (specific stations and years), the

https://doi.org/10.1017/S095410202510028X Published online by Cambridge University Press

Table III. Mean duration in days of the different thermal phases during the study period (2007–2021) at all monitoring stations (letter codes as in Table I; phases: 1 = thawing; 2 = cooling; 3 = attenuation; 4a = isolation; 4b = equilibrium; 5a = melting; 5b = zero curtain), as well as the entire freezing period (F = 2 + 3 + 4a + 4b + 5a + 5b), the snow period (SP = days between snow onset and snow offset) and the snow cover melting (SM = 5a + 5b).

Site	Phase						Period			
	2	3	4a	4b	5a	5b	1	F	SP	SM
JC	48	53	54	2	31	54	115	243	271	85
NI	48	32	48	3	59	98	75	287	300	156
IN	46	75	51	2	36	44	112	253	272	80
CR	60	87	47	0	40	37	94	271	282	77
MO	49	85	65	0	47	40	85	285	283	87
SO	51	126	43	0	54	32	56	306	312	86
LL	45	48	80	18	45	68	67	274	312	113
CL	50	115	34	0	44	27	94	269	277	71

ground reaches the thermal stability phase (Phase 4b) before the snow cover's melting phase (Phase 5a) begins. A gradual rise in temperature characterizes this melting phase until the snowmelt water reaches the ground surface. At this point, temperatures abruptly increase, remaining at ~0°C during the zero-curtain phase (Phase 5b). When the snow finally disappears, the soil starts recording positive temperatures, entering the next summer period (Phase 1).

This progression through the different thermal phases is not consistently observed at all stations throughout the study period. The duration of the phases varies, not only within stations over time, but also between stations (Fig. 5). For example, Phase 1 (warming) lasts 56–115 days (Table III), which is reduced to ~30 days at higher-elevation stations. However, in some years, it can drastically shrink to 15 days, whereas in others, it can extend to as long as 120 days. Phase 2 (cooling) is relatively stable in all stations, with a duration ranging from 45 to 60 days, followed by Phase 3 (attenuation), with more variable durations, ranging from 30 to 120 days. Stations from the Hurd Peninsula at different elevations and geomorphological settings (Table I) showed an apparent increase in the duration of Phase 3 (attenuation) with elevation (JC, NI, IN, CR, MO, SO, from low to high elevation). However, stations in other locations (LL in Byers Peninsula and CL on Deception Island) do not fit that elevation trend (Table III), indicating the impacts of other local thermal behaviour factors on the duration of the thermal phases. The station with the longest duration of Phase 3 (attenuation) is SO at the summit of Reina Sofía Mount. Phase 4a (isolation) typically lasts ~50 days, but at many stations it can extend for more than 100 days (Fig. 5). Phase 4b (equilibrium) is only reached in a few stations in specific years and has a short duration (15–30 days), as observed at LL, where WEqT is reached in various years. The melting (Phase 5a) and zero-curtain (Phase 5b) phases exhibit considerable variability in their duration (Table III), although, on average, the former lasts ~40 days and the latter lasts 50 days on average. In some cases, these phases can extend to as long as 120 days (Fig. 5).

Extreme ground surface temperatures

The annual maximum and minimum GSTs exhibit variability, both over time and among stations (Fig. 6a). Maximum GST ranged from 3.5°C to 23.4°C, with the highest values occurring in 2011 and 2019. In those years, maximum GST ranged between 10°C and 22°C. The minimum values of the GST maxima were reached in 2015, ranging from 4.7°C to 11.8°C. Overall, the maximum GST declined between 2011 and 2015, followed by an increase between 2016 and 2019. In 2020 and 2021, maximum temperatures dropped. The difference in maximum temperatures among stations was ~7–9 °C, with a decrease in temperature with increasing elevation. SO, located at the highest elevation, recorded the lowest maximum temperatures, whereas JC, NI and IN, situated at lower elevations, recorded higher temperatures (Fig. 6a).

The minimum GST exhibits an inverse behaviour to the maxima, although with greater interannual variations. Minimum temperatures are higher when maximum temperatures are lower. In general, minimum GST increased until 2014, declined until 2018 and then rose again (Fig. 6a). The differences between stations range from ~5°C to 10°C. It is worth noting that the highest-elevation station (SO: −12.5°C in 2019) does not record the lowest minimum temperatures in the network; rather, it is CL and CR stations that do so, at −14.8°C and −14.1°C in 2012, respectively.

Considering the limitations of the lack of data from some years due to gaps, the dataset suggests opposite trajectories for both maximum and minimum GSTs calculated for the study period. These trends show a decrease in maximum temperatures and an increase in minimum temperatures (Fig. 6b), although not with equal intensity across all stations. The only exceptions to this behaviour are SO station at the highest elevation, where both maximum and minimum temperatures show decreases, and CR and NI stations, which show slight increases in maximum temperatures. Notably, LL station experiences minimal decreases in maximum temperatures and relatively small increases in minimum temperatures, typically ~2°C per decade.

Although both linear and polynomial fits (Fig. 6) were used to explore the temporal evolution of GST extremes, only the linear regressions were evaluated statistically. Among them, a significant decrease in maximum GST was found at SO station (P = 0.017), whereas no significant trends were detected for the remaining stations or for minimum GST. Polynomial fits, such as that obtained for IN station, were used exclusively to illustrate the apparent cyclicity observed in the interannual variability of extreme values, without indicating statistical significance.

The thermal equilibrium at the end of the winter has never been achieved at the station located on Deception Island (CL). It has

https://doi.org/10.1017/S095410202510028X Published online by Cambridge University Press

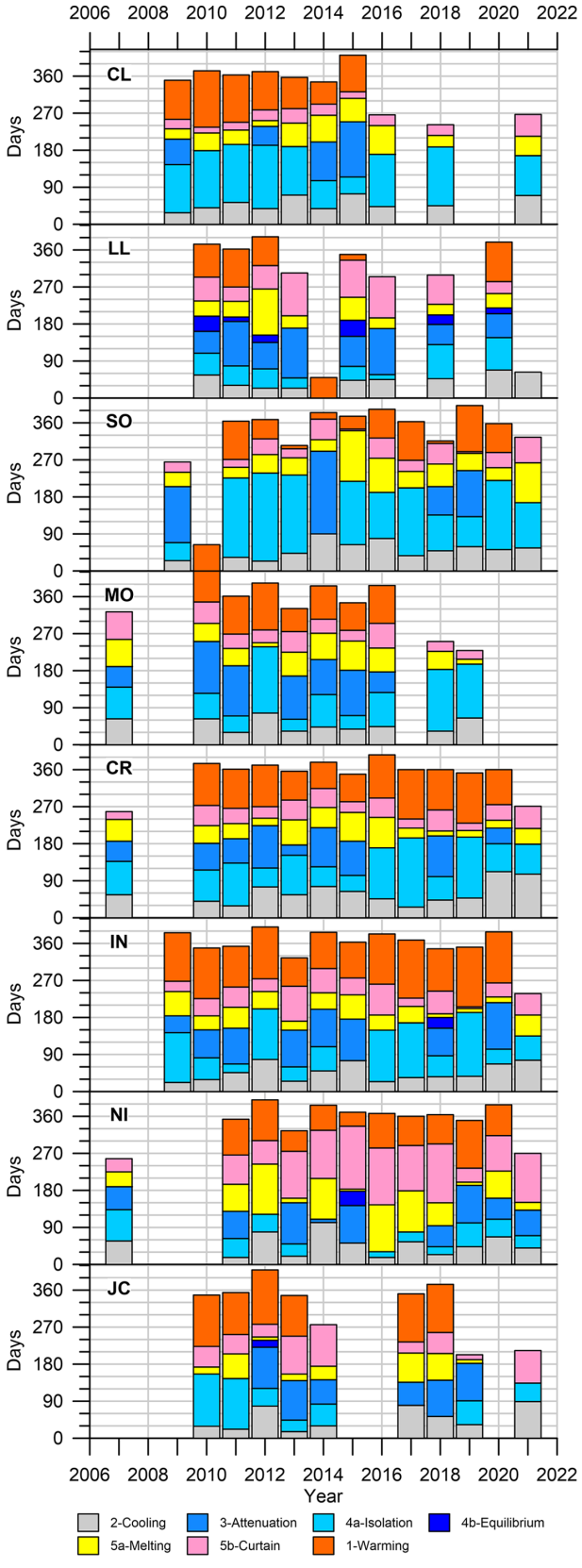

Figure 5. Stacked length in days at the different monitoring stations (letter codes as in Table I) of the different ground thermal phases: 1 = warming (orange), 2 = cooling (grey), 3 = attenuation (bright blue), 4a = insulation (light blue), 4b = equilibrium (dark blue), 5a = melting (yellow) and 5b = zero curtain (pink). Note that one complete period could extend for more than 1 calendar year (i.e. more than 365 days). Incomplete periods are present because data gaps were not assessed in the analysis.

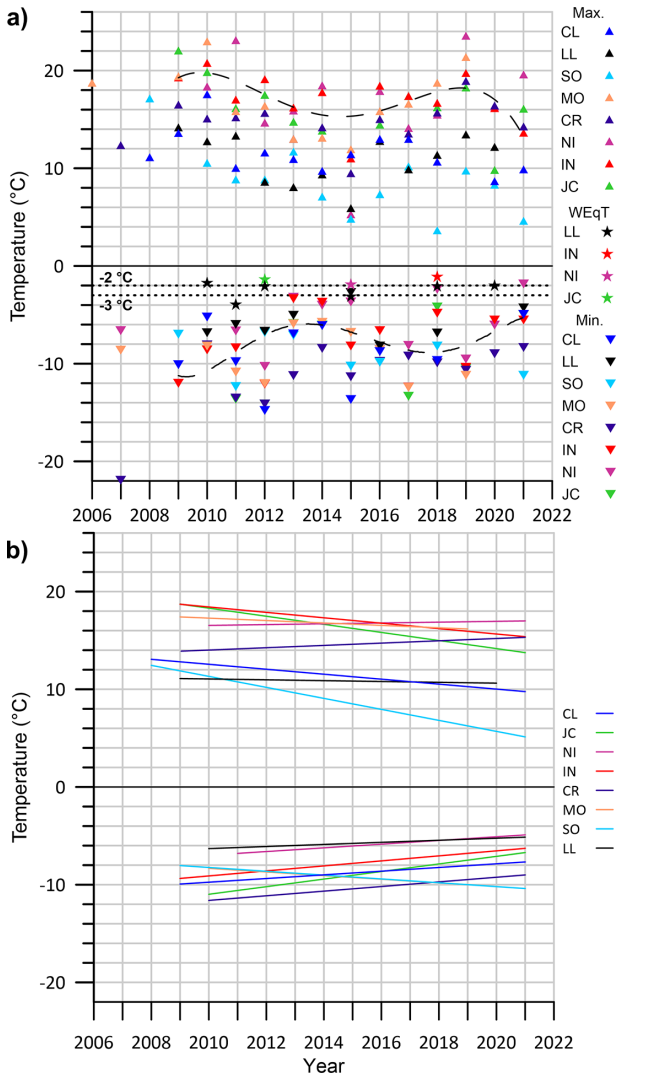

Figure 6. a. Yearly maximum (upward-pointing triangles), minimum (downward-pointing triangles) and equilibrium temperature (WEqT; stars) reached at the different monitoring stations (letter codes as in Table I) during the study period, and polynomial fitting curves (dashed lines) to IN station data showing a cyclical behaviour, as well as their trends. These illustrative polynomial fits are statistically significant ($P < 0.05$), although they are used here solely to highlight the interannual variability at a representative site. Upper (-2°C) and lower (-3°C) WEqT thresholds (dotted lines) for improbable, possible and probable permafrost table presence (Hoelzle 1992) are also shown. **b.** Linear trends of maximum and minimum annual temperatures at each station during the 2007–2021 period. Among the maximum temperatures, only SO station shows a statistically significant trend ($P = 0.017$). Trends in minimum temperatures are not statistically significant at any station ($P > 0.05$).

only been reached once at lower-elevation stations on the Hurd Peninsula of Livingston Island, with very similar temperatures: −1.1°C at JC in 2012, −1.2°C at NI in 2015 and −1.1°C at IN in 2018. However, in Byers Peninsula, thermal equilibrium during the winter has been reached at the LL station on six occasions throughout the study period, with significantly lower temperatures compared to those recorded at the other stations: −1.8°C in 2010, −3.9°C in 2011, −2.1°C in 2012, −3.2°C in 2015, −2.1°C in 2018 and −2.0°C in 2020.

While thermal equilibrium at the end of winter is not attained at all stations in all years due to variation in the snow onset and thickness, in locations where it has been achieved on the Hurd Peninsula of Livingston Island, the WEqT values are at approximately −1°C.

https://doi.org/10.1017/S095410202510028X Published online by Cambridge University Press

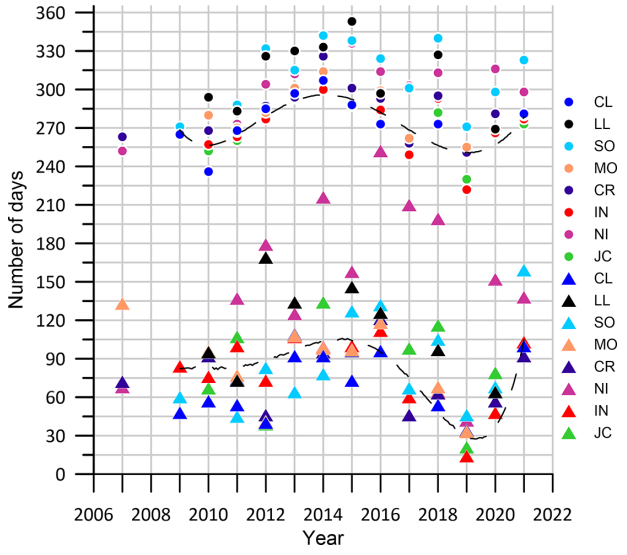

Figure 7. Length in days of the entire snow period (circles) and snow melting (triangles) during the study period at the different ground surface temperature monitoring stations (letter codes as in Table I). A six-degree polynomial fit is shown for the IN station dataset (the most continuous dataset) to illustrate the apparent cyclicity in snow cover duration. The curve is included for descriptive purposes only and was not used for statistical inference.

Snow cover

The duration of the snow-covered period ranges between 240 and 330 days (Fig. 7), with differences of 45–60 days between stations. However, in 2018, this difference exceeded 75 days. Over the years of the study period, the duration of the snow cover on the ground has experienced fluctuations, increasing from 2010 to 2014 and 2015, when it reached its maximum duration at the stations. Then, it decreased again until 2019. Since that year, there has been another increase in duration. Although the time series is very short, an apparent 8 year cycle may be observed, with 2018 standing out as relatively anomalous due to its extended duration of snow cover. Although a six-degree polynomial model was used to illustrate this apparent cyclicity at IN station (Fig. 7), the curve is included for descriptive purposes only. Despite the model yielding a statistically significant fit ($R^2 = 0.81$, $P < 0.0001$), it was not used for inferential analysis due to the limited number of data points and the risk of overfitting.

Within the study period, the duration of the melt-days is much more variable than snow cover duration, both over time and among stations. Generally, the duration of snow cover melt ranges from 15 to 150 days. However, NI station has significantly longer such durations, ranging from 120 to 240 days, with, in general, variability between stations of up to 90 days. The exception is NI station, which shows variabilities of up to 165 days. The melt-phase duration is approximately a third to a quarter of the total snow-covered period. This snowmelt phase also exhibits an apparent cyclical pattern, with a peak in 2014 and 2015 and a minimum in 2019, although this pattern is less distinct than the pattern relating to the snow-covered period duration. Due the numerous stations employed in this analysis across various elevations within the same area, these results demonstrate robustness regarding the observed short-term cycle, despite the brevity of the dataset.

The duration of snow cover varied notably among the years and stations analysed, with longer periods generally observed *ca.* 2014–2015 and shorter durations observed *ca.* 2019 (Fig. 7). Maximum GST values also fluctuated over the study period, with relatively low values recorded in those same years that demonstrated extended or reduced snow cover duration, although this relationship was not consistent across all sites (Fig. 6a).

Discussion

Interannual, seasonal and regional ground surface temperature evolution

The ground surface thermal regimes of the monitoring stations fall under Regime Type 3 (ground cooling before the accumulation of an insulating snow cover; Ishiwaka 2003), indicating that the ground froze during the autumn before the accumulation of sufficient snow to form a thick snow cover layer with insulating capacity. This results in the ground mainly being sensitive to changes in air temperature during the thawing and early freezing periods. These changes in thermal phases observed after 2015 probably reflect the end of the regional cooling period documented in the AP between 2000 and 2015 (Turner *et al.* 2005, 2016, Steig *et al.* 2009, Carrasco 2013, Oliva *et al.* 2017). Despite this temporary cooling, the long-term trend indicates that air temperatures in the AP have continued to rise over recent decades, with its warming rates being among the highest on the continent (González & Fortuny 2018, Turner *et al.* 2019, Bozkurt *et al.* 2020, Carrasco *et al.* 2021, González-Herrero *et al.* 2024). This ongoing warming is expected to further influence the thermal regime of surface soils and the stability of frozen ground in this region (Evtushevsky *et al.* 2020, Carrasco *et al.* 2021, Santamaría-del-Ángel *et al.* 2021, Sato *et al.* 2021). Due to the relatively short time series, it is not possible to establish a direct relationship between the observed fluctuations in snow cover at the stations and the trends of decreasing air temperatures in this Antarctic region between 2000 and 2015, followed by its subsequent increase (e.g. Carrasco 2013, Turner *et al.* 2016, 2019, Oliva *et al.* 2017). This regional trend, however, is not consistently observed across all areas in the region (e.g. de Pablo *et al.* 2024), as is shown in our data (Fig. 7). In fact, we previously described that the trends in snow cover duration (Fig. 7) display a pattern that is the opposite to the variations in maximum GSTs recorded at each station (Fig. 6a). For example, during the years 2014–2015, there was an extended duration of snow cover accompanied by lower maximum temperatures. In contrast, in 2019, when snow cover duration was shorter, lower maximum temperatures were also observed. These observations highlight that the relationship between snow cover and surface temperature is not strictly linear and may be modulated by other local or seasonal factors.

The trend towards the gradual warming of the frozen ground is already evident in the GST data. On the one hand, there is a trend of decreasing maximum temperatures, at least during the study period, alongside an increase in minimum temperatures (Fig. 6), all converging towards temperatures close to 0°C. These results agree with previously identified trends of freeze-thaw indices in the soils and with the number of days under isothermal, freezing and thawing regimes (de Pablo *et al.* 2024), which demonstrated increasing freeze-thaw activity, more frequent isothermal conditions and a progressive convergence of GST values towards 0°C in many of the monitoring sites in the region. Consequently, ground temperatures may also increase following increases in air temperatures, gradually shifting from thermal regimes of Type 3 (ground cooling before the accumulation of an insulating snow cover) to Type 1 (no soil freezing due to the presence of thick snow cover from late summer), or

https://doi.org/10.1017/S095410202510028X Published online by Cambridge University Press

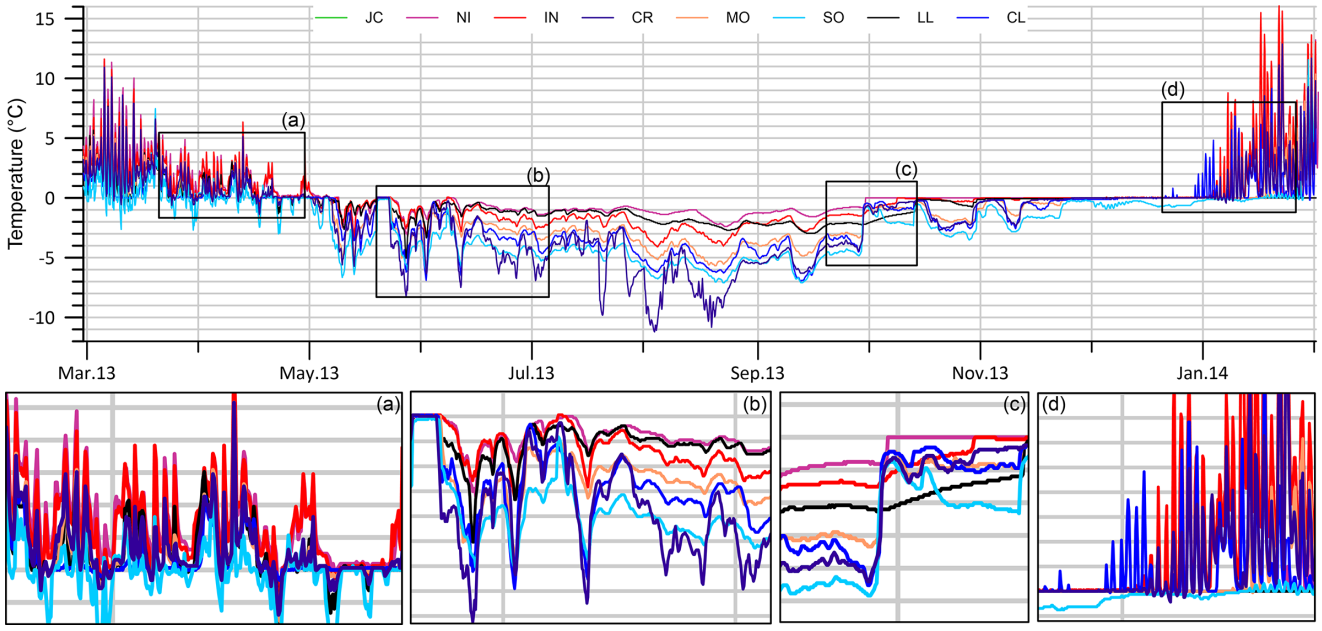

Figure 8. Example of the evolution of ground surface temperature at different monitoring stations (in this case, the 2013–2014 section; letter codes as in Table I), with insets showing **a.** how temperatures show similar behaviour during the thawing period, whereas **b.** temperatures deviate from this general behaviour in late autumn to early winter, **c.** increasing almost at the same time in late winter to early spring and **d.** finishing their zero-curtain period at different dates in summer. The complete thermal record is shown in Fig. 4.

from scenarios with feasible permafrost (possible and/or probable) to others with an absence of permafrost.

A visual comparison of the evolution of the GSTs at the different stations indicates that the temperature regime is very similar during the summer (thawing period; Fig. 4). The most significant differences during the study period (2007–2021) are in the start date of the thawing phase (end of Phase 5b, zero-curtain phase; Fig. 3), the daily thermal variability and the maximum temperatures reached (Fig. 6). This is probably associated with the time it takes for the previous winter's snow cover to disappear completely and with the orographic and altitudinal factors that influence the GST extremes. However, the evolution patterns are comparable (see Fig. 8 as a detailed example of what is shown in Fig. 4), despite the various geological, geomorphological and wind exposure factors at the studied stations (Table I) influencing the energy exchange between the atmosphere and the ground surface.

During the winter (freezing period), the GSTs at all stations appear to exhibits similar behaviour at the beginning of autumn (Fig. 8a). However, the temperatures at different stations gradually deviate from this similar behaviour, becoming less extreme with reduced fluctuations (Fig. 8c). We interpret this behaviour as being due to increasing snow cover, which attains insulating thickness at different times at different stations. During this period, stations that deviate earlier from the general thermal behaviour tend towards thermal regimes of Type 1 (with lower thermal ranges and extended periods of zero curtain; Fig. 2), even if they were originally of Type 3. On the other hand, stations that deviate later from the general trend as the cooling phase progresses align more with Type 3 and eventually with Type 2 thermal regimes.

Snow effects on ground surface temperature

As was introduced in the previous section, the GST regimes appear broadly similar across the studied stations based on visual and numerical comparison, despite differences in elevation and local site characteristics (e.g. topography, geology and grain size; Figs 4 & 8 & Table I). This suggests that additional factors, such as snow cover dynamics, might play a key role in modulating such thermal behaviour. This similarity holds even for stations located at different elevations in the same area, at distant regions on the same island or even on different islands. The effect of snow cover on the ground surface thermal regime has also been described at other sites of the South Shetland Islands. However, although topography appears to play a major role in those areas (Baptista *et al.* 2024), we did not observe any clear topographic influence on the GST regimes at our study sites.

The shift in thermal regime appears to be governed by the arrival of snow cover with insulating capacity. If this cover arrives too early, it prevents ground cooling, leading to higher temperatures and prolonged zero-curtain periods (stations with a Type 3 regime but tending towards a Type 1 regime; Fig. 2). When it arrives too late, temperatures fluctuate significantly and barely have time to reach complete insulation or extended thawing periods (stations with a Type 3 regime but tending towards a Type 2 regime; Fig. 2).

Thus, we can observe how, in general, the station with the most attenuated signal throughout the study period, tending to maintain temperatures only slightly below 0°C (i.e. approaching a Type 1 regime; Fig. 2), is NI station (Table IV). Following in decreasing order of insulation are JC, IN, LL, MO, CR, CL and SO stations. This variability in snow insulation and, consequently, the amount of accumulated snow appears to be more influenced by local topographic setting than by elevation. While CR, MO and SO stations are located at higher elevations and in more exposed areas to the prevailing westerly to north-westerly winds (as reported at nearby meteorological stations; see Bañon & Vasallo 2015), CL station - although at a lower elevation - is also strongly affected by winds due to its unsheltered slope position. In contrast, JC, NI and IN stations are situated at lower elevations and in more sheltered positions. In particular, NI station is protected by surrounding topography and lies at the base of a slope with a south-east aspect. LL station, located at a slightly lower elevation to CR station (Table I), may accumulate more snow due to its location in a depressed area,

https://doi.org/10.1017/S095410202510028X Published online by Cambridge University Press

Table IV. Yearly sequence of stations (letter codes as in Table I) that show the thermal signal's attenuation, marking the beginning of insulation due to thick snow cover. Note that missing station codes indicate gaps in the data for that year at that site or those sites.

Year	Earlier <——————————————————> Later							
2007	NI	MO	CR					
2008								
2009	IN	CR	SO					
2010	JC	LL	IN	MO	CR	CL		
2011	NI	JC	LL	IN	MO	CL	CR	SO
2012	NI	LL	JC	IN	CR	MO	CL	SO
2013	NI	LL	JC	IN	MO	CL	SO	CR
2014	LL	NI	JC	IN	MO	CR	CL	SO
2015	NI	LL	IN	CL	MO	CR	SO	
2016	NI	LL	IN	MO	CL	CR	SO	
2017	NI	JC	IN	MO	CR	SO		
2018	NI	JC	IN	LL	CR	CL	SO	
2019	NI	JC	IN	MO	CR	SO		
2020	NI	LL	IN	CR	SO			
2021	NI	LL	JC	IN	CL	CR	SO	

where snow depths of over 1 m have been reported (e.g. Fassnach *et al.* 2013, de Pablo *et al.* 2014). Due to the relatively thick snow cover, the ground reached thermal equilibrium in several winters during the study period (Fig. 5), and the WEqT range of between −4°C and −2°C is compatible with the presence of permafrost at some stations but not at others.

Examining the sequence in which the stations experience insulating snow cover each year (Table IV), it is evident that NI, LL, JC and IN station are consistently the first to reach this state, whereas MO, CR, CL and SO stations are consistently the last. This suggests that neither site characteristics, such as elevation or wind exposure, nor elevation are entirely determining factors, but that the observed patterns point to snow cover playing the most crucial role during the study period. These results do not imply that topography or other factors might not play a role over the short term, as has been observed in a closed area of the South Shetland Islands (Baptista *et al.* 2024). However, our analysis shows that over the long term, the snow cover variability seems to lead to interannual changes in the ground thermal regime. This also occurred in areas with scarce snow accumulation during winter (Hrbáček *et al.* 2016a), and even during the minor and short-lived snowfalls of the summer season (Hrbáček *et al.* 2016b). This has also been observed to occur in the Northern Hemisphere, where a recent study has demonstrated how different seasonal snow cover levels influence the ground surface thermal regime (Motamedi *et al.* 2024).

Snowmelt and ground surface temperature thermal regime

Despite the differences in location and elevation, it is noteworthy that the date of meltwater percolation into the subsurface is identical at multiple stations or differs by just 1 or 2 days (see Fig. 8c), although in some cases these differences could extend up to 6 days (Fig. 7). This occurs in many years of the studied period, and the differences are smaller between stations located at similar elevations. Only JC station seems to differ from this behaviour, with this probably being due to its early beginning of the melting period (sometimes during late winter) and extensive zero-curtain period (Figs 4 & 5). This suggests that the snow cover begins to thaw almost simultaneously at nearby stations in response to similar environmental conditions, allowing meltwater to rapidly percolate through the snow layer to reach the ground. This is probably due to the relatively high porosity of the snow cover, which, regardless of its thickness, enables rapid water percolation. The duration of the zero-curtain period, if it is related to the snow thickness that needs to thaw at each point, may also be associated with the formation and subsequent thawing of an ice layer between the snow cover and the frozen ground when this water reaches the frozen ground (Zhang 2005). The effects of snowmelt water percolation will have numerous implications for the periglacial processes that may occur, as well as for the mobility of chemical compounds and nutrients (e.g. Chacón *et al.* 2013, Otero *et al.* 2013, Polyakov *et al.* 2020, Gago *et al.* 2023). Thus, in conjunction with the thermal regime itself, snowmelt water percolation will impact the ecology of these Antarctic locations (e.g. Cannone *et al.* 2006, Convey & Smith 2006, Cannone & Guglielmin 2009, Michel *et al.* 2012, Guglielmin *et al.* 2014a, Hrbáček *et al.* 2020).

Ground surface temperature vs permafrost

Permafrost is unlikely at the low-elevation JC, NI and IN stations, in accordance with the probability limits defined in a study of temperatures at the base of snow cover (Hoelzle 1992). These results corroborate findings from other sources and researchers using different datasets (Ferreira *et al.* 2017, de Pablo *et al.* 2024). Conversely, at LL station located in Byers Peninsula, the results indicate values ranging from approximately −4°C to −2°C, suggesting the potential presence of permafrost, in accordance with the previously proposed thresholds (Hoelzle 1992). At stations where this equilibrium temperature has not been achieved, it is not possible to determine the likelihood of permafrost presence using this method, even though at some of them confirmation of this has been obtained through temperature data from boreholes (e.g. SO and CL stations; Ramos *et al.* 2020). This finding agrees with previous studies (de Pablo *et al.* 2014, 2017), including geophysical surveys in similar areas of Byers Peninsula, where sporadic permafrost was described (Correia *et al.* 2017).

Conclusions

The study of the GSTs of the PERMATHERMAL stations on Livingston and Deception islands between 2007 and 2021 allows us to draw the following conclusions:

- Soils exhibit a thermal regime of Type 3 (ground cooling before the accumulation of an insulating snow cover), whereby the ground initially cools during the freezing period due to the absence of snow or its limited thickness. In some cases, the thickness is sufficient to allow the terrain to reach the equilibrium temperature (WEqT).
- Some stations show a regime close to Type 1 (no soil freezing due to the presence of thick snow cover from late summer), although they never reach a fully developed Type 1 regime, indicating a higher presence of snow in those locations.
- Snow is the most critical factor in conditioning the ground surface thermal regime. Stations located at different elevations,

https://doi.org/10.1017/S095410202510028X Published online by Cambridge University Press

in different soils and geomorphological settings and even on different islands exhibit generally similar behaviours during the thawing and the onset of freezing periods, gradually diverging as the snow differentially covers each of them.
- The GST response to snowmelt occurs almost simultaneously at most of the stations, especially if they are close, suggesting that snow thickness is not crucial and that snow allows for percolation, as soil surface warming is almost simultaneous.
- GSTs indicate the absence of permafrost at stations situated at lower elevations (i.e. JC, NI and IN stations). LL station might have permafrost, as shown by the equilibrium temperature ranging between −2°C and −3°C. This classification based on GST thermal regimes and equilibrium temperatures cannot establish the presence of permafrost at the other stations as thermal equilibrium is not reached, but permafrost is known to be present at SO and CL stations, as confirmed by previous studies.
- GST evolution and the duration of snow periods show oscillations, with a cooler peak in 2014 and 2015, when GSTs were at their minimum and snow durations were at their maximum. This is consistent with the cooling in air temperature recorded in the north-western sector of the AP until 2015, followed by subsequent warming.

Supplementary material. To view supplementary material for this article, please visit http://doi.org/10.1017/S095410202510028X.

Acknowledgements. The authors thank the chiefs and crews of the Spanish Antarctic Stations 'Juan Carlos I' on Livingston Island and 'Gabriel de Castilla' on Deception Island for their support during fieldwork and help with instrument' maintenance, as well as the chiefs and crews of the *Las Palmas*, *Hespérides* and *Sarmiento de Gamboa* Spanish research vessels for their support of logistical operations during the 2000–2022 period. The authors also thank their Spanish and Portuguese colleagues who collaborated at the stations in terms of instrument maintenance and data collection. The authors express their gratitude to the two anonymous reviewers for their insightful comments, which significantly contributed to enhancing the quality of the manuscript.

Financial support. This work was supported by the Spanish Research Agency, Ministry of Science, and Innovation, Government of Spain, through the Polar Research Program grants PERMAMODEL (POL2006-01918), PERMAPLANET (CTM2009-10165), ANTARPERMA (CTM2011-15565-E), PERMASNOW (CTM2014-52021-R) projects and PARANTAR (CTM2016-77878-P) projects, as well as PERMATHERMAL contracts with IGME-UAH and CSIC/UTM-UAH LOU art. 83 and LOSU art. 60 UAH PERMATHERMAL 2021/00381, 2022/00102, 2023/00117 and 2024/00041.

Competing interests. The authors declare none.

Author contributions. Conceptualization: MAdP; data acquisition and curation: MAdP and AM; formal analysis: MAdP; funding acquisition: MAdP, MR and JR; investigation: MAdP; methodology: MAdP; project administration: MAdP and MR; resources: MAdP and JR; visualization: MAdP; writing - original draft: MAdP; and writing - review and editing: MAP, MR, GV, AM, JR.

Declaration. During the early preparation of the manuscript, ChatGPT was only used to translate the original text from Spanish to English and for grammar and spelling checking. No text was originally generated using this tool. The manuscript was then carefully discussed, edited and reviewed by all authors.

Research data statement. The data used in this study are publicly available. The raw data are available at the Spanish Polar Data Center (CNDP), and the processed ground temperature data can be obtained from the PERMATHERMAL community in the ZENODO repository at https://zenodo.org, reference number 10.5281/zenodo.8398398, and at the GTN-P database at https://gtnp.arcticportal.org, as well as upon request to the corresponding author.

References

Abram, N.J., Mulvaney, R., Wolff, E.W., Triest, J., Kipfstuhl, S., Trusel, L.D., *et al.* 2013. Acceleration of snow melt in an Antarctic Peninsula ice core during the XX century. *Nature Geoscience*, **6**, 404–411.

Ambrožová, K., Láska, K. & Kavan, J. 2020. Multi-year assessment of atmospheric circulation and impacts on air temperature variation on James Ross Island, Antarctic Peninsula. *International Journal of Climatology*, **40**, 1526–1541.

Auger, M., Morrow, R., Kestenare, E., Sallée, J.-B. & Cowley, R. 2021. Southern Ocean *in-situ* temperature trends over 25 years emerge from interannual variability. *Nature Communications*, **12**, 10.1038/s41467-020-20781-1.

Bañón, M. 1994. El clima en la zona de influencia de la Base Antártica Española 'Juan Carlos I'. *Papeles de Geografía*, **20**, 27–47.

Bañón, M. 2001. *Observaciones meteorológicas en la Base Antártica Española Juan Carlos I. Monografía A-151*. Madrid: Instituto Nacional de Meteorología, Ministerio Medio Ambiente.

Bañon, M. & Vasallo, F. 2015. *AEMET en la Antártida: Climatología y meteorología sinóptica en las estaciones meteorológicas españolas en la Antártida*. Madrid: Agencia Estatal de Meteorología, 150 pp.

Bañón, M., Justel, A., Velázquez, D. & Quesada, A. 2013. Regional weather survey on Byers Peninsula, Livingston Island, South Shetland Islands, Antarctica. *Antarctic Science*, **25**, 146–156.

Baptista, J., Vieira, G. & Lee, H. 2024. Ground surface temperature regimes are controlled by the topography and snow cover in the ice-free areas of Maritime Antarctica. *Catena*, **240**, 10.1016/j.catena.2024.107947.

Bockheim, J., Vieira, G., Ramos, M., López-Martínez, J., Serrano, E., Guglielmin, M., *et al.* 2013. Climate warming and permafrost dynamics in the Antarctic Peninsula region. *Global and Planetary Change*, **100**, 215–223.

Bozkurt, D., Bromwich, D.H., Carrasco, J., Hines, K.M., Maureira, J.C. & Rondanelli, R. 2020. Recent near-surface temperature trends in the Antarctic Peninsula from observed, reanalysis and regional climate model data. *Advances in Atmospheric Sciences*, **37**, 477–493.

Cannone, N. & Guglielmin, M. 2009. Influence of vegetation on the ground thermal regime in Continental Antarctica. *Geoderma*, **15**, 215–223.

Cannone, N., Ellis Evans, J.C., Strachan, R. & Guglielmin, M. 2006. Interactions between climate, vegetation and active layer in Maritime Antarctica. *Antarctic Science*, **18**, 323–333.

Carrasco, J. 2013. Decadal changes in the near-surface air temperature in the western side of the Antarctic Peninsula. *Atmospheric and Climate Sciences*, **3**, 10.4236/acs.2013.33029.

Carrasco, J.F., Bozkurt, D. & Cordero, R.R. 2021. A review of the observed air temperature in the Antarctic Peninsula. Did the warming trend come back after the early 21st hiatus? *Polar Science*, **28**, 100653.

Chacón, N., Ascanio, M., Herrera, R., Benzo, D., Flores, S., Silva, S.J. & García, B. 2013. Do P cycling patterns differ between ice-free areas and glacial boundaries in the Maritime Antarctic region? *Arctic, Antarctic, and Alpine Research*, **45**, 10.1657/1938-4246-45.2.190.

Clem, K.R., Fogt, R.L., Turner, J., Lintner, B.R., Marshall, G.J., Miller, J.R. & Renwick, J.A. 2020. Record warming at the South Pole during the past three decades. *Nature Climate Change*, **58**, 10.1038/s41558-020-0815-z.

Convey, P. & Smith, R.I.L. 2006. Responses of terrestrial Antarctic ecosystems to climate change. *Plant Ecology*, **182**, 1–10.

Convey, P., Bindschadler, R., di Prisco, G., Fahrbach, E., Gutt, J., Hodgson, D.A., *et al.* 2009. Antarctic climate change and the environment. *Antarctic Science*, **21**, 10.1017/S0954102009990642.

Correia, A., Oliva, M. & Ruiz-Fernández, J. 2017. Evaluation of frozen ground conditions along a coastal topographic gradient at Byers Peninsula (Livingston Island, Antarctica) by geophysical and geoecological methods. *Catena*, **149**, 10.1016/j.catena.2016.08.006.

Danby, R. & Hik, D. 2007. Responses of white spruce (*Picea glauca*) to experimental warming at subsurface alpine treeline. *Global Change Biology*, **13**, 437–451.

de Pablo, M.A. 2021. *Maintenance of PT and CALM stations for permafrost and active layer monitoring on Livingston and Deception Islands, Antarctica. 2020–21 campaign report* [in Spanish]. ACMA-Universidad de Alcalá, Alcalá

de Henares, España, 52 pp. Retrived from https://doi.org/10.5281/zenodo.5020140

de Pablo, M.A. 2022. *Maintenance of PT and CALM stations for permafrost and active layer monitoring on Livingston and Deception Islands, Antarctica. 2021–22 campaign report* [in Spanish]. ACMA-Universidad de Alcalá, Alcalá de Henares, España, 55 pp. Retrieved from https://doi.org/10.5281/zenodo.6411073

de Pablo, M.A. 2023. *Maintenance of PT and CALM stations for permafrost and active layer monitoring on Livingston and Deception Islands, Antarctica. 2022–23 campaign report* [in Spanish]. ACMA-Universidad de Alcalá, Alcalá de Henares, España, 66 pp. Retrieved from https://doi.org/10.5281/zenodo.8338315

de Pablo, M.A., Ramos, M. & Molina, A. 2014. Thermal characterization of the active layer at the Limnopolar Lake CALM-S site on Byers Peninsula (Livingston Island), *Antarctica. Solid Earth*, **5**, 10.5194/se-5-721-2014.

de Pablo, M.A., Blanco, J.J., Molina, A., Ramos, M., Quesada, A. & Vieira, G. 2013. Interannual active layer variability at the Limnopolar Lake CALM site on Byers Peninsula, Livingston Island, Antartica. *Antarctic Science*, **25**, 10.1017/S0954102012000818.

de Pablo, M. A., Ramos, M., & Molina, A. 2017. Snow cover evolution, on 2009–2014, at the Limnopolar Lake CALM-S site on Byers Peninsula, Livingston Island, Antarctica. *CATENA*, **149**, 10.1016/j.catena.2016.06.002.

de Pablo, M.A., Ramos, M., Vieira, G., Molina, A., Ramos, R., Maior, C.N., *et al.* 2024. Interannual variability of ground surface thermal regimes in Livingston and Deception islands, Antarctica (2007–2021). *Land Degradation and Devopment*, **35**, 10.1002/ldr.4922.

Delaloye, R. 2004. *Contribution à l'étude du pergélisol de montagne en zone marginale*. GeoFocus, vol 10. Fribourg: Université de Fribourg, 240 pp.

Engel, Z., Laska, K., Nývlt, D. & Stachoň, Z. 2018. Surface mass balance of small glaciers on James Ross Island, north-eastern Antarctic Peninsula, during 2009–2015. *Journal of Glaciology*, **64**, 10.1017/jog.2018.17.

Evtushevsky, O.M., Kravchenko, V.O., Grytsai, A.V. & Milinevsky, G.P. 2020. Winter climate change on the northern and southern Antarctic Peninsula. *Antarctic Science*, **32**, 408–424.

Ferreira, A., Vieira, G., Ramos, M. & Nieuwendam, A. 2017. Ground temperature and permafrost distribution in Hurd Peninsula (Livingston Island, Maritime Antarctic): an assessment using freezing indexes and TTOP modelling. *Catena*, **149**, 10.1016/j.catena.2016.08.027.

Fisher, D.A., Lacelle, D., Pollard, W., Davila, A. & McKay, C.P. 2016. Ground surface temperature and humidity, ground temperature cycles and the ice table depths in University Valley, McMurdo Dry Valleys of Antarctica. *Journal of Geophysical Research - Earth Surface*, **121**, 2069–2084.

Francelino, M.R., Schaefer, C.E.G.R., Simas, F.N.B., Filho, E.I.F., de Souza, J.J.L.L. & da Costa, L.M. 2011. Geomorphology and soils distribution under paraglacial conditions in an ice-free area of Admiralty Bay, King George Island, Antarctica. *Catena*, **85**, 10.1016/j.catena.2010.12.007.

Gago, J., Nadal, M., Clemente-Moreno, M.J., Figueroa, C.M., Barbosa Medeiros, D., Cubo-Ribas, N., *et al.* 2023. Nutrient availability regulates *Deschampsia antarctica* photosynthetic and stress tolerance performance in Antarctica. *Journal of Experimental Botany*, **74**, 10.1093/jxb/erad043.

Gonzalez, S. & Fortuny, D. 2018. How robust are the temperature trends on the Antarctic Peninsula? *Antarctic Science*, **30**, 322–328.

González-Herrero, S., Navarro, F., Pertierra, L.R., Oliva, M., Dadic, R., Peck, L. & Lehning, M. 2024. Southward migration of the zero-degree isotherm latitude over the Southern Ocean and the Antarctic Peninsula: cryospheric, biotic and societal implications. *Science of the Total Environment*, **912**, 10.1016/j.scitotenv.2023.168473.

Goyanes, G.A., Vieira, G., Caselli, A., Mora, C., Ramos, M., De Pablo, M.A., *et al.* 2014. Régimen térmico y variabilidad espacial de la capa activa en isla Decepcion, Antartida. *Revista de la Asociación Geológica Argentina*, **71**, 112–124.

Guglielmin, M. 2006. Ground surface temperature (GST), active layer and permafrost monitoring in Continental Antarctica. *Permafrost and Periglacial Processes*, **17**, 133–143.

Guglielmin, M., Fratte, D. & Cannone, N. 2014a. Permafrost warming and vegetation changes in continental Antarctica. *Environmental Research Letters*, **9**, 10.1088/1748-9326/9/4/045001.

Guglielmin, M., Worland, M.R. & Cannone, N. 2012. Spatial and temporal variability of ground surface temperature and active layer thickness at the margin of Maritime Antarctica, Signy Island. *Geomorphology*, **155**, 20–33.

Guglielmin, M., Worland, M.R., Baio, F. & Convey, P. 2014b. Permafrost and snow monitoring at Rothera Point (Adelaide Island, Maritime Antarctica): implications for rock weathering in cryotic conditions. *Geomorphology*, **225**, 47–56.

Haeberli, W. 1973. Die Basis-Temperatur der winterlichen Schneedecke als möglicher Indikator für die Verbreitung von Permafrost in den Alpen. *Zeitschrift für Gletscherkunde und Glazialgeologie*, **9**, 221–227.

Haeberli, W. 1985. *Creep of mountain permafrost: internal structure and flow of alpine rock glaciers*. Zürich: Mitt. VAW/ETHZ, 142 pp.

Hauck, C., Blanco, J., Gruber, S., Vieira, G. & Ramos, M. 2007. Geophysical identification of permafrost in Livingston Island, Maritime Antarctica. *Journal of Geophysical Research*, **112**, 10.1029/2006JF000544.

Hoelzle, M. 1992. Permafrost occurrence from BTS measurements and climatic parameters in the Eastern Swiss Alps. *Permafrost and Periglacial Processes*, **3**, 143–147.

Hrbáček, F., Láska, K. & Engel, Z. 2016a. Effect of snow cover on the active-layer thermal regime - a case study from James Ross Island, Antarctic Peninsula. *Permafrost and Periglacial Processes*, **27**, 10.1002/ppp.1871.

Hrbáček, F., Cannone, N., Kňažková, M., Malfasi, F., Convey, P. & Guglielmin, M. 2020. Effect of climate and moss vegetation on ground surface temperature and the active layer among different biogeographical regions in Antarctica. *Catena*, **190**, 10.1016/j.catena.2020.104562.

Hrbáček, F., Oliva, M., Láska, K., Ruiz-Fernández, J., de Pablo, M.A., Vieira, G., Ramos, M. & Nývlt, D. 2016b. Active layer thermal regime in two climatically contrasted sites of the Antarctic Peninsula region. *Cuadernos de Investigación Geográfica*, **42**, 10.18172/cig.2915.

IPCC. 2019. *IPCC Special Report on the Ocean and Cryosphere in a Changing Climate* [Pörtner, H.-O., Roberts, D.C., Masson-Delmotte, V., Zhai, P., Tignor, M., Poloczanska, E., *et al.*, *eds*]. Cambridge: Cambridge University Press, 755 pp.

Ishikawa, M. 2003. Thermal regimes at the snow-ground interface and their implications for permafrost investigation. *Geomorphology*, **52**, 105–120.

Kejna, M., Arazny, A. & Sobota, I. 2013. Climatic change on King George Island in the years 1948–2011. *Polish Polar Research*, **34**, 10.2478/popore-2013-0004.

King, L. 1983. High mountain permafrost in Scandinavia. *In PERMAFROST - Fourth International Conference, Proceedings*. Washington, DC: National Academies Press, 612–617.

Lacelle, D., Fisher, D.A., Verret, M. & Pollard, W. 2022. Improved prediction of the vertical distribution of ground ice in Arctic-Antarctic permafrost sediments. *Communications Earth & Environment*, **3**, 31.

Lim, H.S., Kim, H.C., Kim, O.S., Jung, H., Lee, J. & Hong, S.G. 2022. Statistical understanding for snow cover effects on near-surface ground temperature at the margin of Maritime Antarctica, *King George Island. Geoderma*, **410**, 115661.

Meredith, M.P. & King, J.C. 2005. Rapid climate change in the ocean west of the Antarctic Peninsula during the second half of the 20th century. *Geophysical Research Letters*, **32**, 10.1029/2005GL024042.

Michel, R.F.M., Schaefer, C.E.G.R., Poelking, E.L., Simas, F.N.B., Fernandes Filho, E.I. & Bockheim, J.G. 2012. Active layer temperature in two Cryosols from King George Island, Maritime Antarctica. *Geomorphology*, **155–156**, 12–19.

Molina, C., Navarro, F.J., Calvet, J., García-Sellés, D. & Lapazaran, J.J. 2007. Hurd Peninsula glaciers, Livingston Island, Antarctica, as indicators of regional warming: ice-volume changes during the period 1956–2000. *Annals of Glaciology*, **46**, 43–49.

Motamedi, Z., Mattsson, H., Laue, J., Knutsson, S. & Casselgren, J. 2024. Influence of different seasonal snow cover on thermal regime of the ground. *In* Guerra, N., Fernandes, M.M., Ferreira, C., Correia, A.G., Pinto, A. & Pinto, P.S., *eds*, *Geotechnical engineering challenges to meet current and emerging needs of society*. Boca Raton, FL: CRC Press, 3165–3170.

Navarro, F., Jonsell, U., Corcuera, M.I. & Martín, A. 2013. Decelerated mass loss of Hurd and Johnsons glaciers, Antarctic Peninsula. *Journal of Glaciology*, **59**, 10.3189/2013JoG12J144.

https://doi.org/10.1017/S095410202510028X Published online by Cambridge University Press

Obu, J., Westermann, S., Vieira, G., Abramov, A., Balks, M.R., Bartsch, A., *et al.* 2020. Pan-Antarctic map of near-surface permafrost temperatures at 1 km^2 scale. *The Cryosphere*, **14**, 10.5194/tc-14-497-2020.

Oliva, M. & Ruiz-Fernández, J. 2015. Coupling patterns between paraglacial and permafrost degradation responses in Antarctica. *Earth Surface Processes and Landforms*, **40**, 10.1002/esp.3716.

Oliva, M. & Ruiz-Fernández, J. 2017. Geomorphological processes and frozen ground conditions in elephant point (Livingston Island, South Shetland Islands, Antarctica). *Geomorphology*, **293**, 10.1016/j.geomorph.2016.01.020.

Oliva, M., Navarro, F., Hrbáček, F., Hernandéz, A., Nývlt, D., Pereira, P., *et al.* 2017. Recent regional climate cooling on the Antarctic Peninsula and associated impacts on the cryosphere. *Science of the Total Environment*, **580**, 210–223.

Otero, X.L., Fernández, S., de Pablo, M.A., Nizoli, E.C. & Quesada, A. 2013. Plant communities as a key factor in biogeochemical processes involving micronutrients (Fe, Mn, Co, and Cu) in Antarctic soils (Byers Peninsula, Maritime Antarctica). *Geoderma*, **195–196**, 10.1016/j.geoderma.2012.11.018.

Outcalt, S.I., Nelson, F.E. & Hinkel, K.M. 1990. The zero-curtain effect: heat and mass transfer across an isothermal region in freezing soil. *Water Resources Research*, **26**, 10.1029/WR026i007p01509.

Polyakov, V., Abakumov, E. & Mavlyudov, B. 2020. Black carbon as a source of trace elements and nutrients in ice sheet of King George Island, Antarctica. *Geosciences*, **10**, 10.3390/geosciences10110465.

Putzke, J. & Pereira, A.B. 2020. The vegetation of the South Shetland Islands and the climatic change. *In* Kanao, M., Godone, D. & Dematteis, N., *eds*, *Glaciers and the polar environment*. London: InTech, 10.5772/intechopen.94269.

Ramos, M. & Vieira, G. 2009. Ground surface enthalpy balance based on borehole temperatures (Livingston Island, Maritime Antarctic). *Cryosphere*, **3**, 10.5194/tc-3-133-2009.

Ramos, M., Vieira, G., de Pablo, M.A., Molina, A. & Jimenez, J.J. 2020. Transition from a subaerial to a subnival permafrost temperature regime following increased snow cover (Livingston Island, Maritime Antarctica). *Atmosphere*, **11**, 10.3390/atmos11121332.

Ramos, M., Vieira, G., de Pablo, M.A., Correia, A., Molina, A. & Trindade, A. 2013. Análisis del estado térmico del permafrost en las Islas Livingston y Decepción (Antártida). *Proceedings of the IV Iberian Conference of the International Permafrost Association (IPA)*, **42**, 10.13140/2.1.2717.1207.

Ramos, M., Vieira, G., de Pablo, M.A., Molina, A., Abramov, A. & Goyanes, G. 2017. Recent shallowing of the thaw depth at Crater Lake, Deception Island, Antarctica (2006–2014). *Catena*, **149**, 10.3133/of2007-1047srp070.

Ramos, M., Vieira, G., Blanco, J.J., Gruber, S., Hauck, C., Hidalgo, M.A. & Tome, D. 2008a. Active layer temperature monitoring in two boreholes in Livingston Island, Maritime Antarctic: first results for 2000–2006. *In* Kane, D.L. & Hinkel, K.M., *eds*, *Ninth International Conference on Permafrost - extended abstracts*, *June 29–July 3*. Fairbanks, AL: University of Alaska, 1463–1467.

Ramos, M., Vieira, G., Gruber, S., Blanco, J.J., Hauck, C., Hidalgo, M.A., *et al.* 2008b. *Permafrost and active layer monitoring in the Maritime Antarctic: preliminary results from CALM sites on Livingston and Deception Islands*. USGS OF-2007-1047. Short Research Paper 070. Washington, DC: US Geological Survey and the National Academies, 5 pp.

Roberts, J.L., Moy, A.D., Van Ommen, T.D., Curran, M.A.J., Worby, A.P., Goodwin, I.D. & Inoue, M. 2013. Borehole temperatures reveal a changed energy budget at Mill Island, East Antarctica, over recent decades. *The Cryosphere*, **7**, 263–273.

Romanovsky, V.E., Smith, S.L. & Christiansen, H.H. 2010. Permafrost thermal state in the polar Northern Hemisphere during the International Polar Year 2007–2009: a synthesis. *Permafrost and Periglacial Processes*, **21**, 10.1002/ppp.689.

Sancho, L.G., Pintado, A., Navarro, F., Ramos, M., de Pablo, M.A., Blanquer, M., *et al.* 2017. Recent warming and cooling in the Antarctic Peninsula region has rapid and large effects on lichen vegetation. *Scientific Reports*, **7**, 10.1038/s41598-017-05989-4.

Santamaría-del-Ángel, E., Cañon-Páez, M.L., Sebastiá-Frasquet, M.T., González-Silvera, A., Gutierrez, A.L., Aguilar-Maldonado, J.A., *et al.* 2021. Interannual climate variability in the West Antarctic Peninsula under austral summer conditions. *Remote Sensing*, **13**, 1122.

Sato, K., Inoue, J., Simmonds, I. & Rudeva, I. 2021. Antarctic Peninsula warm winters influenced by Tasman Sea temperatures. *Nature Communications*, **12**, 1497.

Savenets, M.V., Pysarenko, L., Krakovska, S., Parnikoza, I. & Pishniak, D. 2023. Local temperature near native vascular plants in the Argentine Islands-Kyiv Peninsula region, Antarctic Peninsula: annual variability and approximation using standard meteorological measurements. *Polar Research*, **42**, 10.33265/polar.v42.8339.

Schoeneich, P. 2011. *Guidelines for monitoring ground surface temperature* (*GST*). PermaNET Alpine Space Project, Italy. 8 pp. Retrieved from https://www.permanet-alpinespace.eu/products/monitoringnetwork/index.html

Smith, M.W. & Riseborough, D.W. 2002. Climate and the limits of permafrost: a zonal analysis. *Permafrost and Periglacial Processes*, **13**, 10.1002/ppp.410.

Steig, E.J., Schneider, D.P., Rutherford, S.D., Mann, M., Comiso, J. & Shindell, D. 2009. Warming of the Antarctic ice-sheet surface since the 1957 IGY. *Nature*, **457**, 459–462.

Turner, J., Colwell, S.R., Marshall, G.J., Lachlan-Cope, T.A., Carleton, A.M., Jones, P.D., *et al.* 2005. Antarctic climate change during the last 50 years. *International Journal of Climatology*, **25**, 279–294.

Turner, J., Maksym, T., Phillips, T., Marshall, G.J. & Meredith, M.P. 2013. Impact of changes in sea ice advance on the large winter warming on the western Antarctic Peninsula. *International Journal of Climatology*, **33**, 10.1002/joc.3474.

Turner, J., Marshall, G.J., Clem, K., Colwell, S., Phillips, T. & Lu, H. 2019. Antarctic temperature variability and change from station data. *International Journal of Climatology*, **40**, 10.1002/joc.6378.

Turner, J., Lu, H., White, I., King, J.C., Phillips, T., Hosking, S.J., *et al.* 2016. Absence of 21st century warming on Antarctic Peninsula consistent with natural variability. *Nature*, **535**, 10.1038/nature18645.

Vieira, G., Hauck, C., Gruber, S., Blanco, J.J. & Ramos, M. 2008. Massive ice detection using electrical tomography resistivity. Examples from Livingston and Deception Islands, Maritime Antarctic. *Proceedings of the VI Assembleia Ibérica de Geofísica*. Retrieved from https://www.researchgate.net/profile/Goncalo-Vieira-4/publication/236606324_Massive_Ice_Detection_using_Electrical_Tomography_Resistivity_Examples_from_Livingston_and_Deception_Islands_Maritime_Antarctic/links/0deec51838cef1c65c000000/Massive-Ice-Detection-using-Electrical-Tomography-Resistivity-Examples-from-Livingston-and-Deception-Islands-Maritime-Antarctic.pdf

Vieira, G., Bockheim, J., Guglielmin, M., Balks, M., Abramov, A.A., Boelhouwers, J., *et al.* 2010. Thermal state of permafrost and active-layer monitoring in the Antarctic: advances during the International Polar Year 2007–2009. *Permafrost and Periglacial Processes*, **21**, 10.1002/ppp.685.

Zhang, T. 2005. Influence of the seasonal snow cover on the ground thermal regime: an overview. *Reviews of Geophysics*, **43**, RG4002.

https://doi.org/10.1017/S095410202510028X Published online by Cambridge University Press